VOLUME 121, NUMBER 14
APRIL 14, 1999

JOURNAL OF THE AMERICAN CHEMICAL SOCIETY

Synthesis and Thermodynamic and Biophysical Properties of Tricyclo-DNA

Ralph Steffens and Christian J. Leumann*,†

Contribution from the Department of Chemistry and Biochemistry of the University of Bern, Freiestrasse 3, CH-3012 Bern, Switzerland

Received October 9, 1998

Abstract: The DNA analogue tricyclo-DNA, built from conformationally rigid nucleoside analogues that were linked via tertiary phosphodiester functions, can efficiently be synthesized from the corresponding phosphoramidites by conventional solid-phase cyanoethyl phosphoramidite chemistry. 5′-End phosphorylated tricyclo-DNA sequences are chemically stable in aqueous, pH-neutral media at temperatures from 0 to 90 °C. Tricyclo-DNA sequences resist enzymatic hydrolysis by the 3′-exonuclease snake venom phosphodiesterase. Homobasic adenine- and thymine-containing tricyclo-DNA octa- and nonamers are extraordinarily stable A-T base-pairing systems, not only in their own series but also with complementary DNA and RNA. Base mismatch formation is strongly destabilized. As in bicyclo-DNA, the tricyclo-DNA purine sequences preferentially accept a complementary strand on the Hoogsteen face of the base. A thermodynamic analysis reveals entropic benefits in the case of hetero-backbone duplex formation (tricyclo-DNA/DNA duplexes) and both an enthalpic and entropic benefit for duplex formation in the pure tricyclo-DNA series compared to natural DNA. Stability of tricyclo-DNA duplex formation depends more strongly on monovalent salt concentration compared to natural DNA. Homopyrimidine DNA sequences containing tricyclothymidine residues form triplexes with complementary double-stranded DNA. Triple-helix stability depends on the sequence composition and can be higher when compared to that of natural DNA. The use of one tricyclothymidine residue in the center of the self-complementary dodecamer duplex (d(CGCGAAT**t**CGCG), **t** = tricyclothymidine) strongly stabilizes its monomolecular hairpin loop structure relative to that of the corresponding pure DNA dodecamer ($\Delta T_m = +20$ °C), indicating (tetra)loop-stabilizing properties of this rigid nucleoside analogue.

Introduction

The use of oligonucleotide analogues as rationally designed drugs continues to attract considerable attention in medicinal chemistry.[1] In the antisense approach,[2] oligonucleotides designed to bind to a given mRNA inhibit the translation process via duplex formation and/or RNase H-induced degradation of the message. In the related antigene approach, oligonucleotides are designed to bind sequence-specifically to double-stranded DNA, thus abolishing gene expression on the level of transcription.[3] A number of first-generation antisense oligonucleotides have been tested in the clinic, and the first oligonucleotide drug, the thiophosphate ISIS-2922, against CMV retinitis was recently admitted to the market.[4] Despite an ongoing debate about the

† Fax: (++41) 31 631 3422. e-mail: leumann@ioc.unibe.ch.

(1) (a) Milligan, J. F.; Matteucci, M. D.; Martin, J. C. *J. Med. Chem.* **1993**, *36*, 1923−1937. (b) Uhlmann, E.; Peymann, A. *Chem. Rev.* **1990**, *90*, 543−584.

(2) De Mesmaeker, A.; Häner, R.; Martin, P.; Moser, H. E. *Acc. Chem. Res.* **1995**, *28*, 366.

(3) (a) Neidle, S. *Anti-Cancer Drug Design* **1997**, *12*, 433−442. (b) Nguyen Thuong, T.; Hélène, C. *Angew. Chem.* **1993**, *105*, 697−723; *Angew. Chem., Int. Ed. Engl.* **1993**, *33*, 666.

(4) (a) Stein, C. A.; Cheng, Y. C. *Science* **1993**, *261*, 1004−1012. (b) Uhlmann, E. *Chem. Zeit* **1998**, *32*, 150−160.

10.1021/ja983570w CCC: $18.00
Published on Web 02/17/1999

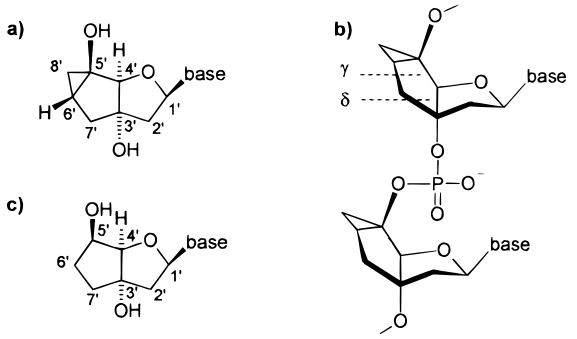

Figure 1. Structures of (a) tricyclonucleoside analogues (base = thymine or adenine), (b) tricyclo-DNA, and (c) bicyclonucleoside analogues.[6]

future of the therapeutic principle in general,[5] the exploration of new concepts in the molecular recognition of RNA and DNA, and with this the generation of new structures exhibiting improved RNA and DNA binding properties and increased biological stability, remains a challenge of general interest.

In extension of our research on the synthesis and properties of oligonucleotides with conformationally restricted sugar−phosphate backbones, we synthesized the nucleic acid analogue tricyclo-DNA (Figure 1). Tricyclo-DNA consists of nucleosides in which the centers C(3′) and C(5′) of the deoxyribofuranose units are linked via an ethylene bridge that is conformationally rigidified by an annelated cyclopropane unit. Tricyclo-DNA is structurally closely related to bicyclo-DNA, which was developed earlier in our laboratory.[6]

The rigid backbone in tricyclo-DNA was designed to explore the influence of structural and conformational preorganization of oligonucleotide single strands on their binding properties. In a preliminary communication,[7] we reported the first results on their base-pairing properties. Here we describe a comprehensive study covering synthesis, duplex and triplex forming properties, and a thermodynamic analysis of duplex formation of a range of tricyclo-DNA sequences containing the nucleobases adenine and thymine.

Results

Synthesis and Enzymatic Stability of Oligo(tricyclodeoxynucleotides). The syntheses of oligo(tricyclodeoxynucleotides) were accomplished on a commercial DNA synthesizer on the 1.0−1.3 μmol scale by standard cyanoethyl phosphoramidite chemistry[8] using the corresponding tricyclo-DNA phosphoramidite building blocks.[9] For synthetic ease, commercially available natural deoxynucleosides immobilized on solid supports were used as starter units. The chain-extension cycles were essentially identical to those for natural oligodeoxynucleotide synthesis[8c] with coupling times of 6 min for tricyclodeoxynucleoside phosphoramidites (for further details, see Experimental Section). The solid support-bound oligomers were obtained with coupling yields of 90−99% per step (trityl assay). The oligo(tricyclodeoxynucleotides) were deprotected and cleaved from the solid support by standard ammonolysis (25% NH_3, 55 °C, ca. 15 h).

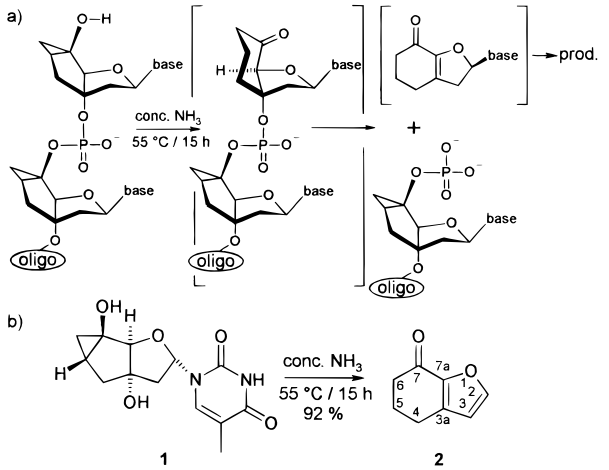

Figure 2. (a) Proposed mechanism of the observed elimination reaction. (b) Model reaction lending support to the mechanism.

During the deprotection step, removal of the 5′-terminal tricyclodeoxynucleoside residue was observed for sequences that were prepared in the trityl off mode (detritylated 5′-terminal hydroxyl group). As a result, the one-unit-shortened, 5′-end phosphorylated oligonucleotides were formed. Due to the presence of the phosphate group, they were chemically stable and no further degradation of the oligonucleotide occurred under the deprotection conditions.

The loss of the 5′-terminal nucleoside unit most probably proceeds via a syn-β-elimination from a ring-enlarged ketone intermediate formed by a thermally induced rearrangement of the cyclopropanol unit under slightly basic, protic conditions (Figure 2 a).[10] Support for this mechanism comes from the model reaction with the nucleoside tricyclo-α-D-thymidine **1** (Figure 2b), which upon treatment with concentrated NH_3 (15 h, 55 °C) afforded 7-oxo-4,5,6,7-tetrahydrobenzofuran **2** in 92% isolated yield.

To obtain the fully modified tricyclo-DNA sequences, the 3′-terminal natural nucleoside unit had to be removed postsynthetically. This was easily achieved by incubation of the corresponding deprotected oligonucleotides with the 3′-exonuclease snake venom phosphodiesterase (SVP). In this way the sequences **5**−**8** (Figure 3) were obtained.

The success of this enzymatic method relies on the striking resistance of tricyclo-DNA to nucleolytic degradation by this enzyme. While the natural DNA sequences $d(A_9)$ and $d(T_9)$ have half-lifes of ca. 5 min when treated with the 3′-exonuclease snake venom phosphodiesterase (SVP) (2 mU/1 OD_{260}) at 37 °C, the corresponding fully modified tricyclo-DNA sequences **6** and **8** showed complete stability under these conditions over several hours, as determined by UV absorption profiles at 260 nm and HPLC- and MALDI-ToF MS analysis.

Crude oligonucleotides and oligonucleotide intermediates were purified by DEAE ion-exchange HPLC. Their purity was controlled by RP-HPLC before subjecting them to routine analysis by MALDI-ToF mass spectroscopy. Figure 3 gives an overview over the oligomers prepared and used in the present

(5) Branch, A. D. *Trends Biochem. Sci.* **1998**, *23*, 45−50.
(6) Tarköy, M.; Bolli, M.; Leumann, C. *Helv. Chim. Acta* **1994**, *77*, 716−744.
(7) Steffens, R.; Leumann, C. *J. Am. Chem. Soc.* **1997**, *119*, 11548−11549.
(8) (a) Sinha, N. D.; Biernat, J.; Köster, H. *Tetrahedron Lett.* **1983**, *24*, 5843−5846. (b) User's Manual, Applied Biosystems PCR-MATE EP DNA Synthesizer (Model 391), 1989. (c) User's Manual (56-1111-56) (Gene Assembler Special/4 Primers) from Pharmacia.
(9) Steffens, R.; Leumann, C. *Helv. Chim. Acta* **1997**, *80*, 2426−2439.
(10) Unsubstituted 1-hydroxybicyclo[*n*.1.0]cycloalkanes (n = 3−6) react in contrast to the here described tricyclonucleosides under similar conditions to α-methylcycloalkanones and not to ring enlarged products (see: Conia, J. M. *Pure Appl. Chem.* **1975**, *43*, 317−326). As ring-opening reactions of cyclopropanols are sensitive to the location and orientation of the substituents (see: Reusch, W.; Grimm, K.; Karoglan, J.; Martin, J.; Subrahamanian, K.; Venkataramani, P. S.; Yordy, J. *J. Am. Chem. Soc.* **1977**, *99*, 1958−1964), the different reactivity might be connected with the substitution pattern at the carbocyclic five-membered ring of the tricyclonucleosides.

		[M-H]⁻ calc.	[M-H]⁻ found
3	d(CGCGAAT**t**CGCG)	3683.5	3683.2
4	d(p**t**T**t**T**t**T**t**T)	2907.0	2908.7
5	d(p**ttttttttt**) = tcd(pT$_8$)	2755.0	2752.8
6	d(p**ttttttttt**) = tcd(pT$_9$)	3097.2	3094.2
7	d(p**aaaaaaaa**) = tcd(pA$_8$)	2827.2	2830.1
8	d(p**aaaaaaaaa**) = tcd(pA$_9$)	3178.3	3182.1
9	d(p**atatatatatT**) = tcd(pAT)$_5$d(T)	3788.3	3790.9
10	d(TTTTT^{Me}C**t**^{Me}CT^{Me}CT^{Me}CT^{Me}CT^{Me}CT)	4533.1	4536.4
11	d(TTT**t**T^{Me}CT^{Me}CT^{Me}C**t**^{Me}CT^{Me}CT)	4571.2	4573.3
12	d(TTT**tt**^{Me}CT^{Me}CT^{Me}CT^{Me}CT^{Me}CT)	4571.2	4575.0
13	d(T**tttt**^{Me}CT^{Me}CT^{Me}CT^{Me}CT^{Me}CT)	4647.2	4646.2
14	d(T**tttt**^{Me}C**t**^{Me}C**t**^{Me}C**t**^{Me}C**t**^{Me}CT)	4799.4	4801.5
15	d(TTTTT^{Me}CT^{Me}CT^{Me}CT^{Me}CT^{Me}CT)	4495.1	4496.3

Figure 3. Synthesized oligonucleotides containing tricyclo-DNA nucleotides (**t** = tcd(T); **a** = tcd(A); ^{Me}C = 5-methyldeoxycytidine).

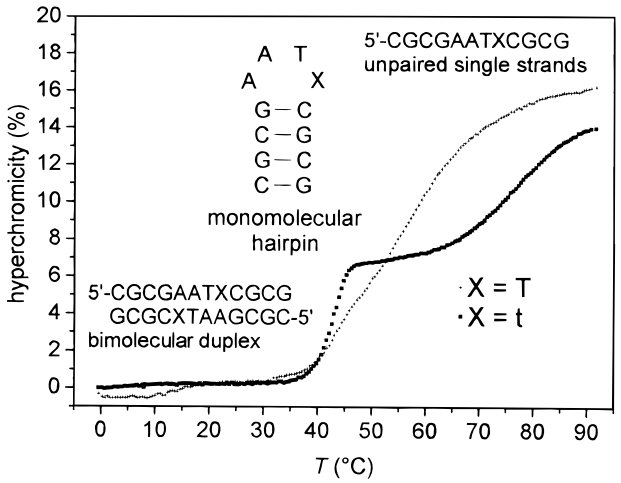

Figure 4. UV melting curves (260 nm) of d(CGCGAATXCGCG) with X = T (thymidine) and X = **t** (tricyclothymidine) in a 10 mM NaH_2PO_4, pH 7.0, 100 mM NaCl buffer, single-strand concentration = 8 μM.

study. All of them were chemically stable under the conditions used for the evaluation of their biophysical properties (HPLC control).

Duplex Formation of DNA Sequences Containing Single and Multiple Tricyclodeoxythymidine Units. The self-complementary dodecamer sequence 5′-CGCGAATTCGCG-3′ can form intramolecular hairpin structures and bimolecular duplexes depending on the solution conditions.[11] At low salt concentrations, both structures coexist and give rise to two transitions in the UV thermal denaturation profile. The transition at lower temperature is concentration dependent and thus reflects the bimolecular duplex melting, while that at higher temperature is concentration invariant and corresponds to the monomolecular hairpin → random coil transition. To evaluate the effect of the substitution of one tricyclothymidine unit (**t**) for a deoxythymidine unit, we prepared the DNA dodecamer d(CGCGAAT-**t**CGCG) **3**. The melting profile (Figure 4) of this sequence revealed that the T_m value (43 °C) of the bimolecular melting process remains unchanged compared to the unmodified sequence d(CGCGAATTCGCG). Surprisingly, however, the transition of the hairpin melting of **3** occurred at 0.1 M NaCl at 77 °C compared to the corresponding T_m value of 57 °C for d(CGCGAATTCGCG). Even under high-salt concentrations (1 M NaCl), where the unmodified sequence exists completely in its duplex form, **3** still exists as a mixture of duplex and hairpin.[12]

Hence, the incorporation of one single tricyclo-DNA nucleotide unit strongly stabilizes the hairpin structure (ΔT_m = +20 °C), without affecting the T_m of bimolecular duplex melting.

In a next step we determined Watson−Crick duplex formation of the noncomplementary sequences **10**−**14**, which vary in the relative amount and the position of the tricyclothymidine units, with their complementary DNA target d((AG)$_5$A$_5$) by UV melting studies at salt concentrations of 150 mM and 1 M NaCl. In these sequences, natural deoxycytidine was replaced by 5-methyldeoxycytidine due to the further use of these sequences for DNA triple-helix formation (vide infra). As shown by UV melting curves (260 nm) at pH 6.0 and 8.0, the affinity of the sequence **14** to the homopurine strand d((AG)$_5$A$_5$) is not pH-dependent. Furthermore the CD spectra of the duplexes **15**·d((AG)$_5$A$_5$) and **14**·d((AG)$_5$A$_5$) (data not shown)[12] are very similar and therefore indicate similar structures for both duplexes. Thus, the alternative reversed Hoogsteen duplex formation as well as triplex formation can be excluded. The melting temperatures (Table 1) show that all sequences **10**−**15** display similar affinities to d((AG)$_5$A$_5$).

Table 1. T_m Values (°C) of the Duplexes of 10−15 with d((AG)$_5$A$_5$) As Determined from UV Melting Curves (λ = 260 nm)[a]

sequence	150 mM NaCl	1 M NaCl
15	54.5	64.2
10	54.4	64.0
11	54.5	64.4
12	55.4	65.3
13	56.4	66.8
14	51.3	64.0

[a] Duplex concentration = 2.8 μM in 10 mm Na_2HPO_4, pH 7.0.

From the inspection of the T_m data, it appears that there exists a weak sequence composition dependence of T_m, favoring consecutive tricyclo-T tracts and disfavoring sequence tracts, where the tricyclo-T units are spaced by natural nucleosides.

Duplex Formation of Fully Modified Tricyclo-DNA Sequences. Complementary pairing experiments of the 5′-end phosphorylated sequences **5**−**8** were carried out in their own series, with the complementary (for synthetic ease non 5′-end phosphorylated) natural DNA sequences d(A$_8$), d(A$_9$), d(T$_8$), and d(T$_9$) and with the RNA polymers poly(A) and poly (U) at high (1 M) and low (150 mM) NaCl concentrations. Neither sequence, tcd(pT$_9$) **6** and tcd(pA$_9$) **8**, showed any cooperative melting transition at the temperature interval of 0−90 °C without complement. Thus, self-association of **6** or **8** could be excluded. All melting temperatures are summarized in Table 2, and representative melting curves of DNA−RNA hybrid complexes are depicted in Figure 5.

At 150 mM NaCl, both tricyclo-DNA sequences, tcd(pT$_9$) **6** and tcd(pA$_9$) **8**, show increased T_m values compared to their natural counterparts d(T$_9$) and d(A$_9$) when paired to the RNA polymers poly(A) and poly(U). The higher stability of the complexes tcd(pA$_9$)·poly(U) and tcd(pT$_9$)·poly(A) is indicated by ΔT_m values of +16 and +15 °C, respectively, relative to the natural reference complexes. The pairing behavior of the tricyclo-DNA 8-mers tcd(pT$_8$) **5** and tcd(pA$_8$) **7** with RNA is analogous to that of the corresponding 9-mers.

With complementary DNA, the duplexes containing a tricyclopyrimidine strand, tcd(pT$_9$)·d(A$_9$) and tcd(pT$_8$)·d(A$_8$), are

(11) Marky, L. A.; Blumenfeld, K. S.; Kozlowski, S.; Breslauer, K. J. *Biopolymers* **1983**, *22*, 1247−1257.

(12) Steffens, R. Dissertation, Universität Bern, in preparation.

Table 2. T_m Values (°C) from UV Melting Curves (260 nm) in a 0.15 M NaCl (1 M NaCl in Parentheses) Buffer[a]

	tcd(pA_8) **7**	tcd(pA_9) **8**	d(A_8)	d(A_9)	poly(A)
tcd(pT_8) **5**	46 (61)		4 (24)		27 (39)
tcd(pT_9) **6**		52 (72)		12 (31)	35 (44)
d(T_9)		34 (48)		16 (24)	20 (32)
d(T_8)	28 (40)		8 (14.5)		16 (28)
4		15 (40)		6 (27)	8 (27)
poly(U)	43 (66)	48 (73)	31 (52)	32 (53)	60 (76)

[a] 10 mM NaH_2PO_4, pH 7.0, duplex concentration = 4.6 μM (melting experiments with RNA: total base-pair concentration = 41−43 μM).

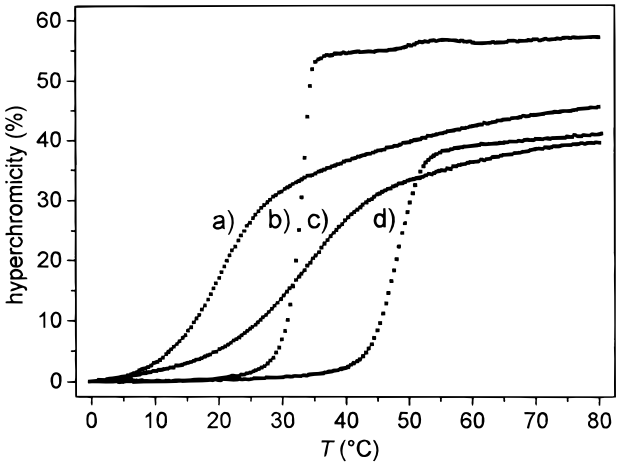

Figure 5. UV melting profiles (260 nm) of (a) d(T_9)·poly(A), (b) d(A_9)·poly(U), (c) tcd(pT_9)·poly(A), and (d) tcd(pA_9)·poly(U) in 10 mm NaH_2PO_4, pH 7.0, 150 mM NaCl, total base-pair concentration = 41−43 μM.

slightly less stable than the corresponding natural duplexes (ΔT_m = −4 °C) at low salt conditions. Inversely, the duplexes containing a tricyclo-DNA purine strand, tcd(pA_9)·d(T_9) and tcd(pA_8)·d(T_8), show considerably increased melting temperatures (ΔT_m values of +18 °C and +20 °C, respectively). In its own series, the tricyclo-DNA duplexes tcd(pT_9)·tcd(pA_9) and tcd(pT_8)·tcd(pA_8) are the most stable pairing systems with T_m's of 52 and 46 °C (ΔT_m = +36 and +38 °C, respectively). The possibility of T−A·T triplex formation in 1:1 stoichiometric mixtures of tcd(pA_9) with d(T_9) or tcd(pT_9) was ruled out earlier.[7] Interestingly, sequence **4**, which consists of alternating d(T) and tcd(T) units, displays a pronounced sensitivity to the ionic strength of the buffer solution. While the duplex **4**·d(A_9) is slightly more stable than the DNA reference (ΔT_m = +3 °C) at 1 M NaCl, its stability is significantly decreased at 150 mM NaCl (ΔT_m = −10 °C). This compares well with observations made with sequence **14** and reflects again the reduced affinity for mixed-backbone sequences with a high number of natural-to-tricyclonucleoside steps within the chain.

The differentially higher thermodynamic stability of duplexes containing tricyclo-DNA purine strands was also demonstrated in a polyacrylamide gel shift competition experiment. In a 1:1:1 mixture of the 9-mers d(A_9) and d(T_9) and the tricyclo-DNA homopurine sequence tcd(pA_9) **8**, the more stable duplex d(T_9)·tcd(pA_9) is formed exclusively, leaving behind d(A_9) as a single strand (Figure 6, lane 5). The preferred formation of the duplex d(T_9)·tcd(pA_9) is in agreement with the thermodynamic data of duplex formation obtained from UV melting curves (vide infra).

Hoogsteen Selectivity of Tricyclo-DNA Purine Sequences. The CD spectrum of tcd(pT_9)·tcd(pA_9)[7] is very similar to that

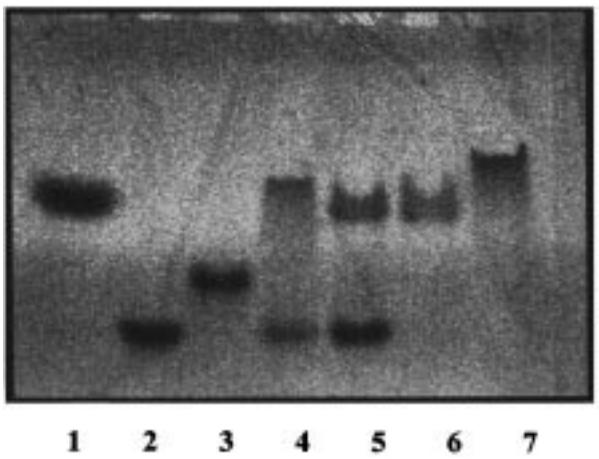

Figure 6. UV shadowing of a nondenaturing 18% polyacrylamide gel. Buffer: 89 mM Tris·borate (pH 8.1), 10 mM $MgCl_2$. The samples were dissolved in 15 μL of loading buffer (8% sucrose, 10 mM $MgCl_2$, 89 mM Tris·borate) and stored at room temperature for 30 min before loading on the gel. The gel was run at 80 V for 13 h at 4 °C: lane **1**, Xylenecyanol FF; **2**, d(A_9); **3**, tcd(pA_9); **4**, d(T_9)·d(A_9); **5**, d(T_9)·d(A_9) + 1 equiv of tcd(pA_9); **6**, d(T_9)·tcd(pA_9); **7**, d(T_9):d(A_9) 2:1.

Table 3. ΔT_m Values (°C) from UV Melting Curves (260 nm) of Mismatched Relative to Matched Duplexes[a]

ΔT_m	d(A_4XA_4) or d(T_4XT_4)			
X =	T	dA	dC	dG
d(T_9)	−19.5	0	−18.7	−18.9
tcd(pT_9)	−20.1	0	−23.0	−19.8
d(A_9)	0	−21.0	−21.0	−21.0
tcd(pA_9)	0	−28.0	−29.7	−35.0

[a] c = 4.3 μM in 10 mM NaH_2PO_4, pH 7.0, 1 M NaCl. Duplex partner sequences were either d(A_4XA_4) or d(T_4XT_4), where X represents one of the three remaining natural nucleotide units.

of a corresponding bicyclo-DNA duplex[13] and quite different from that of d(T_9)·d(A_9). From this we conclude that, in analogy to bicyclo-DNA, the homobasic purine containing tricyclo-DNA sequences form preferentially a Hoogsteen or reverse-Hoogsteen duplex and not a Watson−Crick duplex. Further evidence for this binding mode arises from experiments with the sequence tcd(pAT)$_5$d(T) (**9**), which does not show any cooperative melting behavior. A−T alternating sequences are complementary systems according to the Watson−Crick base-pairing mode, but they are incompatible with the Hoogsteen and/or the reverse-Hoogsteen base-pairing mode, provided that all glycosidic torsion angles between the base and the sugar units are in the anti-conformational range. As in the case of bicyclo-DNA, this change in pairing preference is most likely due to the geometric shift of the backbone torsion angle γ relative to that observed in natural DNA duplexes.[13]

Pairing Selectivity. To examine the effect of base mismatches on duplex stability, we recorded UV melting curves of tricyclo-DNA·DNA hybrid duplexes containing a single mismatched base pair in the center. Both sequences, the tricyclo-DNA 9-mer tcd(pT_9) and for comparison the natural sequence d(T_9), were paired with d(A_4XA_4), where X represents each of the four natural nucleosides T, dA, dC, and dG. As can be seen from the corresponding ΔT_m values (Table 3), the melting temperatures decrease in both, the hybrid and the natural series, to an almost equal extent ($\Delta T_m \approx -20$ °C).

When the purine oligomers tcd(pA_9) and d(A_9) were paired with the corresponding 9-mers d(T_4XT_4), a different picture

(13) Bolli, M.; Litten, C.; Schütz, R.; Leumann, C. *Chem. Biol.* **1996**, *3*, 197−206.

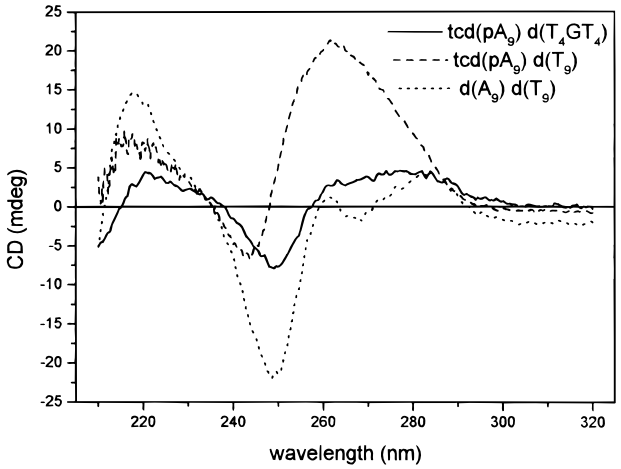

Figure 7. CD spectra of the matched duplexes tcd(pA_9)·d(T_9) and d(A_9)·d(T_9) and the mismatched duplex tcd(pA_9)·d(T_4GT_4) in 10 mM NaH_2PO_4, pH 7.0, 1 M NaCl, $T = 0$ °C.

Table 4. Thermodynamic Data of Duplex Formation Obtained from UV Melting Curves (T_m^{-1} vs ln(c) Plots) in a 10 mM NaH_2PO_4, pH 7.0, 1 M NaCl Buffer

	ΔH [kcal mol^{-1}]	ΔS [cal K^{-1} mol^{-1}]	ΔG^{25} [kcal mol^{-1}]
d(A_9)·d(T_9)	−53.8	−154.6	−7.7
d(A_9)·tcd(pT_9)	−41.4	−109.1	−8.8
tcd(pA_9)·d(T_9)	−47.2	−121.3	−11.0
tcd(pA_9)·tcd(pT_9)	−59.6	−147.6	−15.5

appears (Table 3). While the duplexes in the natural series d(A_9)·d(T_4XT_4) show ΔT_m values of ca. −21 °C per mismatch, ΔT_m's of −28 to −35 °C were observed in the hybrid series tcd(pA_9)·d(T_4XT_4). The CD spectrum of the duplex tcd(pA_9)·d(T_4GT_4), as an example, shows all the characteristics of a Watson−Crick base-paired structure, while the completely matched sequence tcd(pA_9)·d(T_9) is typical for a Hoogsteen base-paired structure[13] (Figure 7). Thus, introduction of a mismatch in this hybrid system seems to be associated with a change of the base-pairing mode from the preferred Hoogsteen to the Watson−Crick mode. Since duplex formation, regardless of its structure, is expected to be under thermodynamic control, and due to the fact that no mismatched Hoogsteen duplex is formed, we conclude that in the Hoogsteen base-paired structures, mismatch discrimination is much stronger than in the Watson−Crick base-paired structures. Whether this is a general phenomenon also valid in natural nucleic acid association remains to be shown.

Thermodynamic Data of Duplex Formation. Thermodynamic data of duplex formation were obtained from DNA melting curves by the concentration variation method.[14] The data obtained from plots of $1/T_m$ vs ln(c) of the four duplexes d(A_9)·d(T_9), d(A_9)·tcd(pT_9), tcd(pA_9)·d(T_9), and tcd(pA_9)·tcd(pT_9) (see Supporting Information) are summarized in Table 4.

The net value of the pairing entropy ΔS is lower for all duplexes in which tricyclo-DNA sequences are involved. This indicates that the entropy term of duplexation contributes to a stabilization of the corresponding duplexes. The lower (less negative) value for the pairing enthalpy ΔH for d(A_9)·tcd(pT_9) and tcd(pA_9)·d(T_9) on the other hand goes along with a destabilization of the hybrid duplexes. The extraordinary stability of the tricyclo-DNA duplex tcd(pA_9)·tcd(pT_9) is the result of not only an entropic but also enthalpic stabilization. A direct comparison of thermodynamic data of tcd(pA_9)- with d(A_9)-containing duplexes, however, is compromised by the two different duplex structures formed (Hoogsteen and Watson−Crick, respectively). The calculated standard enthalpies of duplex formation $\Delta G^{25°C}$correspond to the observed melting behavior at 1 M NaCl, in which the natural DNA duplex d(A_9)·d(T_9) shows the lowest melting temperature.

Salt Concentration Dependence of Duplex Formation. An investigation of the dependence of the melting temperature upon the NaCl concentration yields a linear relationship between T_m and ln[NaCl] (see Supporting Information). Comparison of the slopes of these curves indicates a stronger dependence of T_m from the salt concentration in the case of the tricyclo-DNA duplex tcd(pA_9)·tcd(pT_9) ($\partial T_m/\partial$ ln[NaCl] = 10.5) than for the natural duplex d(A_9)·d(T_9) ($\partial T_m/\partial$ ln[NaCl] = 4.5). We calculated the change in countercation uptake (Δn) for both duplexes, d(A_9)·d(T_9) and tcd(pA_9)·tcd(pT_9), according to the polyelectrolyte theory[15] (eq 1) using the duplex formation enthalpies ΔH from Table 4.

$$\Delta n = -\frac{\partial T_m}{\partial \ln[\mathrm{NaCl}]}\frac{2\Delta H^0}{RT_m^2} \quad (1)$$

The substantially higher differential cation screening in the case of the tricyclo-DNA duplex tcd(pA_9)·tcd(pT_9) ($\Delta n = 5.9$) compared to d(A_9)·d(T_9) ($\Delta n = 2.9$) is not only due to the additional two 5′-terminal phosphate groups in the former duplex but is also connected with more condensed negative charges in the tricyclo-DNA duplex. This is well explained by the structural difference of the Hoogsteen duplex tcd(pA_9)·tcd(pT_9) vs the Watson−Crick duplex d(A_9)·d(T_9). From structural models it is clear that in a Hoogsteen duplex the backbones of the two complementary strands are much nearer together in space, and therefore suffer from a higher electrostatic repulsion, than in a Watson−Crick duplex.

Triplex Formation. To explore the double-strand affinity of oligonucleotides containing tricyclic nucleotide units, we investigated the triplex-forming properties of the 15-mer sequences **10**−**14**, in which thymidine is replaced at different positions by tricyclothymidine units (Figure 3). These sequences were designed to bind in the parallel binding mode to the 21-mer DNA target duplex d(GCTAAAAAGAGAGAGAGATCG)·d(CGACTCTCTCTCTTTTTTAGC). The natural 2′-deoxycytidine nucleotides in the third strand sequences were replaced by 5-methyl-2′-deoxycytidine to facilitate triplex formation at neutral pH. The sequence d(T_5(^{Me}CT)$_5$) (**15**) was used as reference strand. T_m data of third strand dissociation are summarized in Table 5.[16] As expected, triplex stability is pH-dependent in all cases due to the need of protonation of the third strand ^{Me}C residues.

Triple helices of the target duplex with sequence **14**, containing four tricyclothymidine units in a row and four tricyclothymidine units spaced by ^{Me}C units, show the lowest triplex stability with ΔT_m values between −4.5 °C (pH 6.5) and −7.2 °C (pH 7.5) compared to 15-mer **15**. The highest T_m's were obtained with the oligomer **13**, in which 4 of the 5 consecutive thymidine units are replaced by tricyclothymidine.

(14) Marky, L. A.; Breslauer, K. J. *Biopolymers* **1987**, *26*, 1601−1620.

(15) Cantor, C. R.; Schimmel, P. R. *Biophysical Chemistry Part III: The Behavior of Biological Macromolecules*, W.H. Freeman & Co.: New York, 1980; pp 1135−1141.

(16) The melting profiles were recorded in a buffer (140 mM KCl, 7 mM Na_2HPO_4, 0.5 mM $MgCl_2$) which approximates the intracellular cationic environment (see: Alberts, B.; Bray, D.; Lewis, J.; Raff, M.; Roberts, K.; Watson, J. D. *Molecular Biology of the Cell*, 3rd ed.; Garland: New York, 1994; p 508).

Table 5. T_m Values (°C) and Hyperchromicity (%) (in Parentheses) of the Dissociation of the Third Strand from the Target Duplex As Determined from UV Melting Curves ($\lambda = 260$ nm)[a]

strand	pH 6.5	pH 7.0	pH 7.5
15	43.0 (7)	31.4 (6)	20.9 (3)
10	41.7 (9)	29.5 (5)	19.7 (3)
11	41.7 (6)	29.2 (6)	19.0 (3)
12	45.6 (6)	33.1 (6)	22.2 (4)
13	47.5 (7)	35.0 (5)	24.1 (4)
14	38.5 (7)	25.7 (4)	13.7 (2)

[a] Triple helix concentration 1.5−1.7 μM in 140 mm KCl, 7 mM Na_2HPO_4, 0.5 mM $MgCl_2$. T_m of the target duplex: 57.5 ± 1 °C.

At pH 7.0 both the triple helices with the sequences **12**, containing two adjacent tricyclo-T residues, and **13** are stabilized with a ΔT_m/ modification of +0.9 °C compared to the unmodified sequence **15**. These results show that there exists a sequence composition effect which might reflect sequence-dependent differences in conformation of the target duplex and/or third strand. Notably, a similar behavior was observed in Watson−Crick duplex formation of the sequences **10**−**15** (vide supra).

Discussion

The key features of tricyclo-DNA, as known so far, are (i) the ease of synthesis via phosphoramidite chemistry, despite its structural complexity, (ii) its resistance toward nucleolytic enzymes, (iii) its hairpin-loop stabilizing properties, and (iv) the strong hybridization properties of homobasic A- and T-containing sequences with complementary RNA.

The successful incorporation of tricyclic adenosine and thymidine analogues into oligonucleotides shows again that standard phosphoramidite oligonucleotide synthesis is compatible with building blocks showing sterically hindered, tertiary hydroxy functions. This is a further demonstration of the tolerance for structural variations in the corresponding building blocks and thus underlines again its general synthetic value for the preparation of carbohydrate-modified oligonucleotides.

While bicyclo-DNA sequences are still substrates for enzymatic degradation with exo- and endonucleases, the addition of the cyclopropyl ring in tricyclo-DNA brings about almost complete resistance against the 3′-exonuclease SVP. Since 3′-exonuclease activity is mostly responsible for the degradation of oligonucleotides in human and murine sera,[17] this property is of considerable value in regard to a potential use of tricyclo-DNA in a biological environment.

An interesting and largely unrecognized feature of structurally rigid nucleosides is their use for the stabilization of secondary structural motifs. We have shown that replacement of only one natural thymidine unit in the tetraloop hairpin structure of the self-complementary sequence 5′-CGCGAATTCGCG-3′ by tricyclothymidine (sequence **3**) changes its T_m by 20 °C toward higher temperatures. Hence, it is conceivable that loops, similar to those involved in the catalytic core of ribozymes[18] or the recently described DNA enzymes,[19] could be stabilized by incorporation of nucleoside analogues with geometrically suitable, fixed carbohydrate structures. This might constitute one way of improving the performance of such catalysts.

Homobasic tricyclo-DNA sequences are extraordinarily stable A-T base pairing systems. The increase in T_m/modification is by + 4 °C (150 mM NaCl) and + 5 °C (1 M NaCl) higher in the case of the tricyclo-DNA than for the recently investigated hexitol nucleic acids (HNA), which display ΔT_m/modification values of ca. + 3 °C for oligo(A)·oligo(T) duplexes.[20] This is additional evidence for the fact that structural preorganization can substantially increase complex stability, even in nucleic acid analogues with a charged phosphodiester backbone. Other oligonucleotide analogues that can also be regarded as members of the family of conformationally restricted oligonucleotides[21] and that form complexes of similar stability are p-RNA[22] and the recently introduced analogue "locked nucleic acid" (LNA).[23]

As in the case of bicyclo-DNA, we attribute the change in the association preferences (Watson−Crick vs Hoogsteen) to the structural alteration of the backbone torsion angle γ which deviates from its normal range of 54° (average) in B-DNA[24] to ca. 150° (estimated from molecular modeling) in bicyclo-DNA[13] and to ca. 120° (estimated from molecular modeling) in tricyclo-DNA.[9] From this we conclude that the change of −30° in γ between bicyclo-DNA and tricyclo-DNA is not enough to bring about a phosphodiester backbone conformation that prefers Watson−Crick base pairing.

The tricyclo-DNA duplexes investigated were thermodynamically more stable than the corresponding bicyclo-DNA duplexes. Thus, the introduction of the cyclopropyl ring has a further stabilizing effect. While increased stability is reflected in the reduced entropy terms in duplex formation, there is also a distinct stabilizing enthalpy term in the pure tricyclo-DNA duplex that is absent in the corresponding pure bicyclo-DNA duplex. This might be the result of less geometric strain within the given base-pairing arrangement in the tricyclo-DNA duplex.

A higher hybridization affinity with natural DNA sequences is a prerequisite for potential strand-displacement or strand-invasion processes.[25] Effective strand-invasion to form D-loop structures was recently shown for peptide−nucleic acid (PNA) sequences[26] and for oligonucleotides containing phosphoramidate linkages.[27] Oligonucleotide analogues capable of strand invasion are of interest in the modulation of gene expression, e.g., as transcription promoters.[28]

Of further interest is the strongly enhanced base-pairing selectivity observed by pairing of the tricyclopurine sequence **8** to a DNA complement with a mismatched base in the center of the sequence, compared to the corresponding natural DNA sequence. A likely interpretation of this fact is that Hoogsteen duplex formation is more selective toward complementary base-pair formation than Watson−Crick duplex formation. This

(17) Eder, P. S.; DeVine, R. J.; Dagle, J. M.; Walder, J. A. *Antisense Res. Dev.* **1991**, *1*, 141−151.
(18) (a) McKay, D. *RNA* **1996**, *2*, 395−403. (b) Cate, J. H.; A. R. Gooding, Podell, E.; Zhou, K.; Golden, B. L.; Kundrot, C. E.; Cech, T. R.; Doudna, J. A. *Science* **1996**, *273*, 1678−1685.
(19) Santoro, S. W.; Joyce, G. F. *Proc. Natl. Acad. Sci. U.S.A.* **1997**, *94*, 4262−4266.
(20) Hendrix, C.; Rosemeyer, H.; Verheggen, I.; Seela, F.; Van Aerschot, A.; Herdewijn, P. *Chem. Eur. J.* **1997**, *3*, 110−120.
(21) Kool, E. T. *Chem. Rev.* **1997**, *97*, 1473−1487.
(22) Pitsch, S.; Wendeborn, S.; Jaun, B.; Eschenmoser, A. *Helv. Chim. Acta* **1993**, *76*, 2161−2183.
(23) (a) Obika, S.; Nanbu, D.; Hari, Y.; Andoh, J.; Morio, K.; Doi, T.; Imanishi, T. *Tetrahedron Lett.* **1998**, *39*, 5401−5404. (b) Singh, S. K.; Nielsen, P.; Koshkin, A. A.; Wengel, J. *Chem. Commun.* **1998**, 455−456. (c) Koshkin, A. A.; Singh, S. K.; Nielsen, P.; Rajwanshi, V. K.; Kumar, R.; Meldgaard, M.; Olsen, C. E.; Wengel, J. *Tetrahedron* **1998**, *54*, 3607−3630.
(24) Saenger, W.; *Principles of Nucleic Acid Structure*; Springer-Verlag: New York, 1984.
(25) Nielsen, P. E.; Egholm, M.; Berg, R. H.; Buchardt, O. *Science* **1991**, *254*, 1497−1500.
(26) Demidov, V. V.; Yavnilovich, M. V.; Belotserkovskii, B. P.; Frank-Kamenetskii, M. D.; Nielsen, P. E. *Proc. Natl. Acad. Sci. U.S.A.* **1995**, *92*, 2637−2641.
(27) Zhou-Sun, B.; Sun, J.; Gryaznov, S. M.; Liquier, J.; Garestier, T.; C. Hélène, Taillandier, E. *Nucleic Acids Res.* **1997**, *25*, 1782−1787.
(28) Møllegaard, N. E.; Buchardt, O.; Egholm, M.; Nielsen, P. E. *Proc. Natl. Acad. Sci. U.S.A.* **1994**, *91*, 3892−3895.

finding is of interest in the context of earlier observations on bimolecular triplex formation in the parallel mode with cyclic oligonucleotides, where also a higher mismatch discrimination was found.[29] In these cases, however, only double mismatch situations on both, the Watson−Crick and the Hoogsteen side of a purine base were investigated.

In summary, tricyclo-DNA is a new, conformationally rigid DNA analogue with interesting and unusual supramolecular association properties and with potentially useful biological properties.

Experimental Section

Enzymes. Phosphodiesterase from *Crotalus durissus* and alkaline phosphatase from calf intestine were from Böhringer Mannheim. HPLC: Pharmacia-LKB-2249 gradient system attached to an ABI-Kratos-Spectroflow-757 UV/VIS detector and a Tarkan W + W 600 recorder. Extinction coefficients ϵ_{260} of d(A_8) (82 500), d(A_9) (92 700), d(AAAAAGAGAGAGAGA) (179 900), d(T_8) (66 400), d(T_9) (74 400), and d(TTTTT^{Me}CT^{Me}CT^{Me}CT^{Me}CT^{Me}CT) (107 400) were determined as described;[30] ϵ_{260} of d(GCTAAAAAGAGAGAGAGATCG) (184 600) and of d(CGATCTCTCTCTCTTTTTAGC) (196 500) were available.[31] The same extinction coefficients were used for both, DNA and tricyclo-DNA. UV melting curves: Varian Cary-3E UV/VIS spectrometer equipped with a temperature-controller unit and connected to a Compaq-ProLinea-3/25-zs personal computer; at temperature gradients of 0.5 °C/min, data points were collected in intervals of ca. 0.3 °C, and at temperatures <20 °C, the cell compartment was flushed with N_2 to avoid condensation of H_2O on the UV cells. %Hyperchromicity (wavelength) = 100[$D(T) - D_0$]/D_0 with $D(T)$ = absorption at temperature T and D_0 = lowest absorption in the temperature interval; the transition temperature T_m was determined as described.[14]

Elimination Reaction: 7-Oxo-4,5,6,7-tetrahydrobenzofuran (= 5,6-Dihydro-4*H*-benzofuran-7-one) (2). The α-anomeric tricyclic nucleoside **1** (18 mg, 64 μmol) was dissolved in concentrated NH_3 (1 mL) and left for 21 h in a sealed Eppendorf tube at 55 °C. After complete evaporation of the solvent, the residual product was purified by flash chromatography (5 g of silica gel, hexane:ethyl acetate 3:1) to yield 8 mg (92%) of the ring-enlarged elimination product **2** as a slightly yellow solid, R_f 0.58 (hexane:2-propanol 3:1). Mp: 56−57 °C. UV/VIS (methanol): λ_{max} (ϵ) = 269 (14 880). ^{1}H NMR (300 MHz, DMSO-d_6): δ 7.93 (d, ^3J(H,H) = 1.83 Hz, 1 H; H-C(2)), 6.63 (d, ^3J(H,H) = 1.83, 1 H; H-C(3)), 2.72 (t, ^3J(H,H) = 5.88, 2 H; H_2C(6)), 2.44 (t, ^3J(H,H) = 7.35, 2 H; H_2C(4)), 2.02 (quint, ^3J(H,H) = 5.88, 2 H; H_2C(5)). ^{13}C NMR (75 MHz, $CDCl_3$, multiplicities from DEPT spectra): δ 186.17 (s, C(7)), 147.72 (s, C(7a)), 147.33 (d, C(2)), 139.87 (s, C(3a)), 111.49 (d, C(8)), 38.25 (t, C(6)), 24.42 (t, C(4)), 22.94 (t, C(5)). IR (film): 2924, 2853, 2360, 2341, 1674, 1433, 1412, 1297, 1108, 1002, 892, 782, 668 cm^{-1}. MS (EI): *m/z* (rel intensity) 136 (100, M^+), 121 (30), 108 (76), 80 (23), 52 (21).

The spectroscopic data are identical with those described for 7-oxo-4,5,6,7-tetrahydrobenzofuran.[32]

Synthesis of Oligo(tricyclodeoxynucleotides). Syntheses of oligonucleotides were performed with solid-phase phorsphoramidite methodology on the 1.3 μmol scale using a Pharmacia LKB Gene Assembler Special instrument connected to a Compaq-ProLinea-3/25-zs personal computer. For the synthesis on the 1.0 μmol scale of **3**, an Applied Biosystems PCR-MATE EP DNA Synthesizer (Model 391) was used. Reagent solutions were prepared according to the manufacturers protocols,[8b,c] with the exception of 1*H*-tetrazole (0.45 m solution in MeCN) which was from Fluka. MeCN was distilled over CaH_2 and stored under activated molecular sieves (3 Å). The assembly of tricyclo-DNA was performed according to the standard synthesis cycles[8b,c] with the exception of a prolonged coupling time (6 min), an 11-fold instead of a 9-fold excess of phosphoramidites, and the use of a 0.07 M instead of a 0.1 M solution of the tricycloadenosine building block due to its poor solubility. Either LCAA-CPG (Sigma) or polystyrene (Pharmacia) bound natural nucleosides were used as starter units. If not stated otherwise, all syntheses were performed in the trityl off mode, ending with 5′-detritylated oligomers. Coupling efficiencies as monitored by on-line trityl assay were between 90 and 99%. After synthesis, the solid support was suspended in concentrated NH_3 solution (ca. 1 mL) and left for 15 h at 55 °C or 2 h at room temperature for the synthesis of sequence **6**. The crude oligonucleotides were purified by ion-exchange HPLC on a Nucleogen DEAE 60-7 (125 × 4 mm) column (Macherey & Nagel). The isolated oligonucleotides were desalted over SEP-PAK C-18 cartridges (Waters) according to a standard procedure.[33] Synthesis data of the sequences **3**−**14** are summarized in Table 6 (Supporting Information). The corresponding MS data are in Figure 3. All natural oligodeoxynucleotides that were used for comparison of biophysical properties were synthesized according to the standard procedure and purified by DEAE-HPLC.

General Procedure for the Enzymatic Removal of the 3′-Terminal Natural Thymidine Units. The purified oligodeoxynucleotides (7 OD_{260}) were dissolved in 150 mm NaCl, 10 mm Tris·HCl, pH 7.0 (1 mL) and incubated with 3 μL of alkaline phosphatase (1 mg/mL) and 3 μL of phosphodiesterase (2 mg/mL) at 37 °C. After 5 h, this solution was subjected to HPLC purification.

Acknowledgment. This work was supported by a grant of the Swiss National Science Foundation.

Supporting Information Available: Listing of UV melting curves of the duplex **6·8** and the sequence **9** (Figure 8) and of the triple helices of **13**, **14**, and **15** with the 21-mer DNA target duplex (Figure 9), $1/T_m$ vs ln(c) plots of d(A_9)·d(T_9), d(A_9)·**6**, d(T_9)·**8**, and **6·8** (Figure 10), T_m vs ln[NaCl] plots of d(A_9)·d(T_9) and **6·8** (Figure 11), and synthesis and analytical data of oligo(tricyclodeoxynucleotides) (Table 6) (PDF). This material is available free of charge via the Internet at http://pubs.acs.org.

JA983570W

(29) Kool, E. T. *J. Am. Chem. Soc.* **1991**, *113*, 6265−6266.
(30) Bolli, M.; Lubini, P.; Leumann, C. *Helv. Chim. Acta* **1995**, *78*, 2077−2096.
(31) Plum, G. E.; Park, Y.-W.; Singleton, S. F.; Dervan, P. E.; Breslauer, K. J. *Proc. Natl. Acad. Sci. U.S.A.* **1990**, *87*, 9436−9440.
(32) Walsh, E. J., Jr.; Stone, G. B. *Tetrahedron Lett.* **1986**, *27*, 1127−1130.
(33) Sambrook, J.; Fritsch, E. F.; Maniatis, T. *Molecular Cloning: A Laboratory Manual*; Cold Spring Harbor Laboratory Press: Plainview, NY, 1989; p 11.29.